Theoretical study of dilute GaN–4d transition metal alloys

2006 J. Phys.: Condens. Matter 18 8589

(http://iopscience.iop.org/0953-8984/18/37/017)

INSTITUTE OF PHYSICS PUBLISHING JOURNAL OF PHYSICS: CONDENSED MATTER

J. Phys.: Condens. Matter **18** (2006) 8589–8601 doi:10.1088/0953-8984/18/37/017

Theoretical study of dilute GaN–4d transition metal alloys

R de Paiva[1], **R A Nogueira**[1] **and J L A Alves**[2]

[1] Departamento de Física, Universidade Federal de Minas Gerais, CP 702, 30123-970, Belo Horizonte, MG, Brazil
[2] Departamento de Ciências Naturais, Universidade Federal de São João del Rei, CP 110, 36301-160, São João del Rei, MG, Brazil

Received 16 March 2006, in final form 21 July 2006
Published 1 September 2006
Online at stacks.iop.org/JPhysCM/18/8589

Abstract

Electronic calculations were carried out for the dilute ordered alloys $Ga_{0.94}(TM)_{0.06}N$ (TM = Y, Zr, Nb, Mo, Tc, Ru, Rh, Pd, and Ag) in the zinc-blende structure. The theoretical framework used was the density functional theory, using the local spin density approximation, as implemented in the full-potential linearized augmented plane wave method. We examine energy band structures, densities of states, charge distributions, and local magnetic moments and anticipate the properties of these promising systems for applications in spin electronic devices.

(Some figures in this article are in colour only in the electronic version)

1. Introduction

The III nitride compounds are semiconductor materials that look promising for use in optoelectronics and spintronics. Their equilibrium phase has the wurtzite structure; however the zinc-blende structure, very close in energy, has many advantages for device applications, may be obtained by means of non-equilibrium processes of crystal growth, and has merited intensive experimental and theoretical studies [1–3]. Previously, we have studied the dilute magnetic semiconductors (DMS) $Ga_{1-x}Mn_xN$ and $Al_{1-x}Mn_xN$ and the related compound MnN in the zinc-blende phase [2, 3]; these compounds are of great interest nowadays due to their potentialities in the fabrication of semiconductor devices which make use of the spin property of the charge carriers. Earlier, Sato *et al* [5] have studied theoretically the dilute alloys made with GaN, in the wurtzite structure, doped with the 3d transition metals V, Cr, Mn, Fe, Co, and Ni. In the present work we examine the electronic and magnetic properties of ordered dilute alloys based on GaN, in the zinc-blende phase, doped with 4d transition metal atoms (4d TM) substituting for Ga in a concentration $x = 6\%$. This study is stimulated both by the results already found for $Ga_{1-x}Mn_xN$ [2] and $Al_{1-x}Mn_xN$ [3] and by the fast developing technology based on III nitrides. On the other hand, the actual mechanisms supporting the ferromagnetism induced by the carriers in the dilute alloys based on GaN are still not well

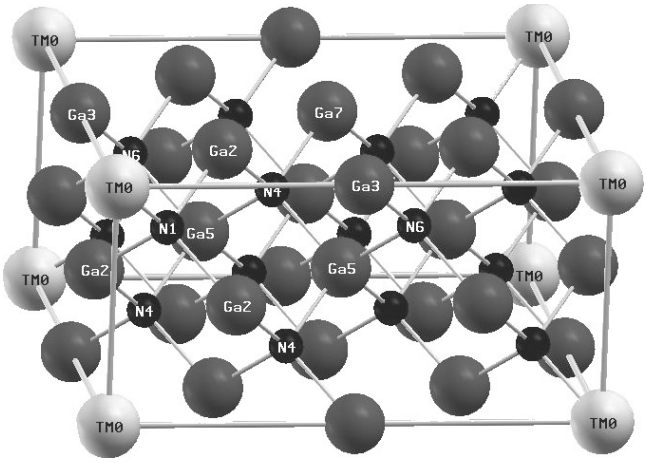

Figure 1. The 32-atom supercell used to simulate the ordered alloys with zinc-blende structures. The numbering of the atoms follows the ordering of the shells of neighbours around the transition metal atom TM0.

understood. Therefore, we think that a systematic theoretical study of the electronic and magnetic properties of the whole series of dilute Ga(4d TM)N alloys are of great interest.

2. Theoretical framework

We carry out first-principles, spin-polarized calculations using the full-potential linear augmented plane wave (FP-LAPW) method within the local spin density functional approximation (LSDA) [6]. In particular, we use the FP-LAPW method as implemented in the Wien2k code [7]. In this method, the unit cell is divided, in a muffin-tin geometry, into (I) non-overlapping atomic spheres (centred at the atomic sites) and (II) an intersphere (interstitial) region in order to generate the set of basis functions. Inside an atomic sphere, the basis set is described by a linear combination of radial functions times spherical harmonics, and in the interstitial region is described using plane waves. We use the Ceperley–Alder data [8] for the exchange–correlation energy of the homogeneous gas as parametrized by Perdew and Wang [9]. The core states are calculated fully relativistically (retaining only the spherical part of the potential), whereas we include only scalar relativistic effects (without spin–orbit interaction) for all valence states (including the 4d TM and 4d Ga states). The valence part is treated with the potential expanded into spherical harmonics up to $l = 6$, while the valence wavefunctions inside the spheres are expanded up to $l = 10$. In all cases we use an APW + lo orbital [10, 11] type of basis with an additional local orbital for the 4s TM and 4p TM semi-core states.

Muffin-tin radii equal to 1.06 and 0.87 Å for cations (Ga and TM) and anions, respectively, are chosen so that the atomic spheres touch each other. The basis set size is fixed by choosing the FP-LAPW parameter $RK_{max} = 7.0$. In the calculations we use the tetrahedron method on a grid of 12 k-points in the irreducible part of the Brillouin zone, which corresponds to 100 k-points in the whole Brillouin zone, in order to make the numerical integrations. In figure 1, we show the supercell containing 32 atoms in the zinc-blende structure, used in the calculations. The ordering of the atoms follows the ordering of the shells of neighbours around the transition metal atom labelled TM0 (N1 means the first shell of nitrogen atoms, Ga2 the second shell of the gallium atoms, etc). The zinc-blende structure is composed of two face-centred cubic

Table 1. Lattice parameters, a_0 (Å), for (4d TM)N and Ga(4d TM)N alloys in the zinc-blende structure.

	Y	Zr	Nb	Mo	Tc	Ru	Rh	Pd	Ag
(4d TM)N	5.19	4.90	4.70	4.58	4.50	4.47	4.51	4.62	4.79
Ga(4d TM)N	4.51	4.50	4.48	4.48	4.47	4.47	4.47	4.48	4.49

(fcc) lattice displaced from each other by a quarter of a body diagonal. The Ga atoms are placed on one fcc lattice and the N atoms on the other fcc lattice. In order to simulate the alloys ($x = 0.06$), we replace one Ga atom in the unit cell by one TM atom. Self-consistency was achieved by demanding the convergence of both the total energy and the eigenvalues to be smaller than 10^{-6} eV.

In table 1 we show the lattice parameters of the alloys that we used in the calculations. They were obtained by using Vegard's law [12], as applied to the binary components GaN ($a_0 = 4.46$ Å) and (4d TM)N (table 1), whose lattice parameters were determined by means of the total energy calculations using the same theoretical approach[3].

3. Electronic properties

3.1. Energy band structures

We display in figure 2 the spin-polarized energy bands calculated along the main symmetry directions in the Brillouin zone. These bands, as analysed at the Γ point, can be separated into the following parts: (i) narrow energy bands around −16.8 eV (Y); −18.5 eV (Zr); −18.4 eV (Nb); −18.2 eV (Mo); −17.9 eV (Tc); −17.8 eV (Ru); −17.2 eV (Rh); −16.7 eV (Pd); and −16.1 eV (Ag), having an average width around 1.0 eV originating from the 2s N states; (ii) energy bands centred at −14.1 eV (Y); −15.7 eV (Zr); −15.5 eV (Nb); −15.2 eV (Mo); −14.8 eV (Tc); −14.7 eV (Ru); −14.2 eV (Rh); −13.7 eV (Pd); and −13.1 eV (Ag), having an average width around 2.5 eV originating from the 3d Ga states; (iii) wide bands located in the ranges −8.19 to 2.46 eV (Y); −9.87 to 0.24 eV (Zr); −9.71 to −0.07 eV (Nb); −9.43 to 0.06 eV (Mo); −8.98 to 0.38 eV (Tc); −8.91 to 0.07 eV (Ru); −8.31 to 0.04 eV (Rh); −7.86 to −0.12 eV (Pd); −7.39 to −0.02 eV (Ag), having an average width ∼7.0 eV which are built up mainly of 4s Ga, 4p Ga and 2p N; (iv) bands with energies higher than 2.9 eV (Y); 1.2 eV (Zr); 1.3 eV (Nb); 1.4 eV (Mo); 1.7 eV (Tc); 1.5 eV (Ru); 1.9 eV (Rh); 2.2 eV (Pd); 2.7 eV (Ag), constituting the conduction band of the GaN and originating from the 4s Ga and 4p Ga states; (v) states close to the bottom of the conduction band and to the Fermi level which originate from the 4d TM states.

[3] Using this procedure we are supposing that there is a homogeneous distribution of the transition metal inside the GaN matrix, without changing the zinc-blende structure. Vegard's law has been shown to apply to bulk dilute magnetic materials such as $Ga_{1-x}Mn_xAs$ [13–15]; recently, it has been proven to apply also to a range of doped II–VI semiconductor quantum dots [16–19]. Of course, breaks from the linearity can arise due to a structural phase transition or, in extreme cases, due to phase segregation, which leads to the observation of both the bulk guest and the bulk host lattices in, for instance, x-ray diffraction data. The introduction of an impurity, like Mn, into a host matrix (for instance GaAs, InAs, and GaN) is expected to disrupt the local atomic structure around the impurity. This disruption may alter the electronic structure significantly if it is associated with symmetry lowering. However, pseudopotential first-principles calculations carried out for the dilute systems $Ga_{1-x}Mn_xAs$ and $In_{1-x}Mn_xAs$ [20], and $Ga_{1-x}Mn_xN$ [21, 22], allowing for local atomic relaxations, revealed that relaxation effects on the computed atomic structure were small (keeping the local tetrahedral symmetry) and on the electronic structure were negligible. We use these facts as a guide for our model calculation to study the similar systems $Ga_{1-x}(4d\ TM)_xN$; as our all-electrons method is computationally more demanding than the pseudopotential methods, we adopt Vegard's law (based on first-principles calculations of the lattice parameters of the binary compounds) in order to define an appropriate parameter for the ideally ordered dilute alloys.

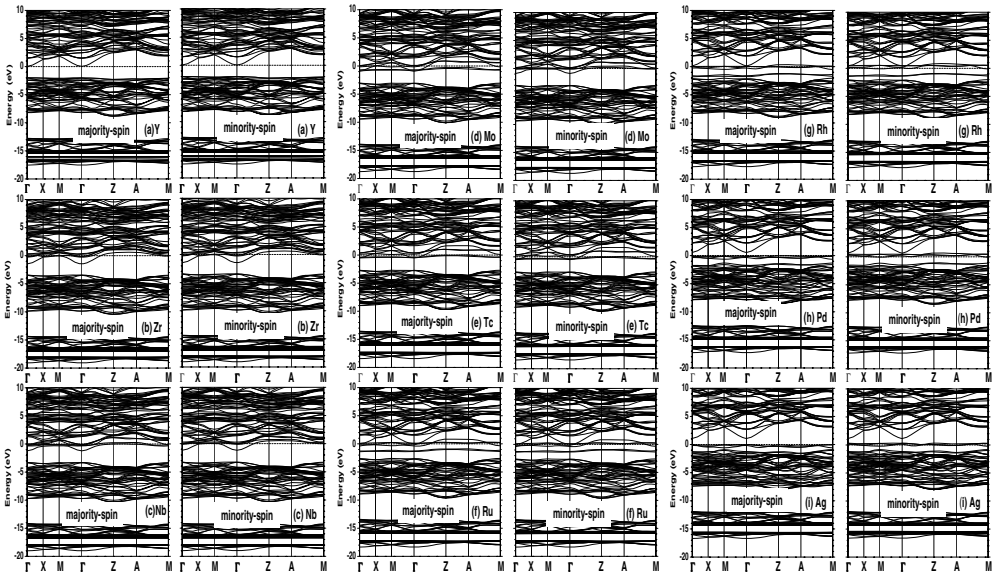

Figure 2. Spin-polarized band structures of $Ga_{0.94}(4d\ TM)_{0.06}N$ along selected high symmetry directions. The energy zero is chosen to be at the Fermi energy.

In what follows we analyse the 4d TM bands. The atomic 4d states in the zinc-blende structure are split by the crystal field into states of symmetries e (doubly degenerate) and t_2 (triply degenerate). We can see that: (i) for the alloy GaYN there is no spin polarization, there is some (2p N)–(4d TM) hybridization with the top of the valence band (VB) of the GaN, the 4d Y states are unoccupied and localized at high energies in the conduction band (CB) of the GaN; (ii) for GaZrN there is also no spin polarization, there is some hybridization with the top of the VB, and the bottom of the CB is occupied. There are 4d(e) Zr states close to the bottom of the CB; (iii) in the case of GaNbN there is spin polarization, there is occupation of the bottom of the CB and of the majority spin 4d(e) Nb states, the $4d(t_2)$ Nb states are scattered in the CB and there occurs a small (2p N)–(4d TM) hybridization with the VB; (iv) for GaMoN there is still spin polarization occurring, occupation of the bottom of the CB and of 4d(e) Mo states, and majority spin states close to the bottom of the CB; there are unoccupied 4d(e) Mo states and semi-occupied $4d(t_2)$ Mo states; (v) in the case of GaTcN, again, there is no spin polarization, all 4d(e) Tc states are occupied, and there are $4d(t_2)$ Tc unoccupied states close to the bottom of the CB; (vi) for GaRuN there is still no spin polarization, there is total occupation of the 4d(e) Ru states, of the bottom of the CB, of some of the $4d(t_2)$ Ru, and there is a small hybridization with the VB; (vii) in the case of GaRhN, there occurs spin polarization, all 4d(e) Rh states are occupied and localized inside the fundamental gap of GaN, there are $4d(t_2)$ Rh semi-occupied states, just entering the gap, and $4d(t_2)$ Rh spin minority unoccupied states close to the Fermi level. There is hybridization with the VB; (viii) the spin polarization remains in the case of GaPdN, 4d(e) Pd occupied states appear inside the VB, the $4d(t_2)$ Pd majority spin states are totally occupied inside the gap, there are unoccupied $4d(t_2)$ Pd spin minority states close to the Fermi energy. There is hybridization with the VB; (ix) finally, in the GaAgN alloy there is still spin polarization, the 4d(e) Ag states are totally immersed in the VB, the $4d(t_2)$ Ag majority spin states are totally occupied, the spin minority states are semi-occupied and both are inside the gap. There is hybridization with the VB. Making an overall synthesis of the evolution of the

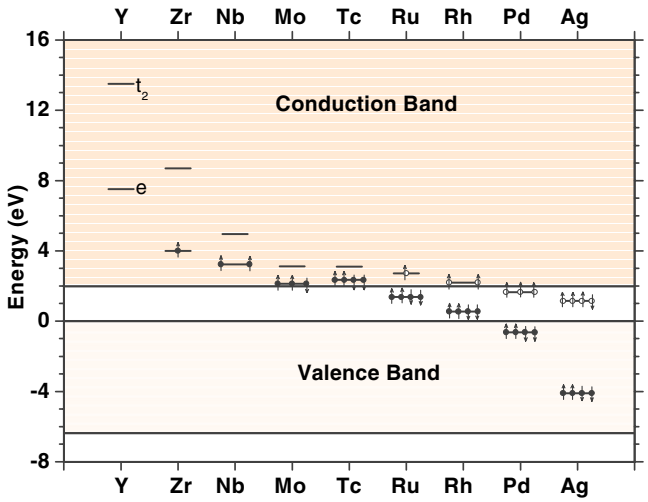

Figure 3. The evolution along the series of the energy levels introduced by the transition metals, at the Γ point, as referred to the top of the valence band of GaN. The open circles indicate the occupations of the e states (full circles) and of the t_2 states (open circles). The arrows indicate the spin states.

energy levels associated with the transition metal, we can identify the following behaviour. In the case of Y, the conduction band is unoccupied, there is no spin polarization and the 4d states are localized at high energies in the CB. For Zr, the extra electron is located at the bottom of the conduction band (at the position of the Fermi energy), and as this state is delocalized, there is no spin polarization. For Nb, one of the extra electrons, occupying the bottom of the CB, pairs to the other electron occupying a localized 4d(e) state and induces a spin polarization. This spin polarization remains for Mo and disappears for Tc, when the electrons occupy all the four available 4d(e) states. In the case of Ru, four electrons occupy the 4d(e) Ru states and the remaining electron occupies a delocalized state, at the bottom of the CB, without causing a spin polarization. For Rh, besides the four electrons occupying the 4d(e) states, two electrons are paired, occupying 4d(t_2) states, near the bottom of the CB and inducing a spin polarization; this polarization increases in the case of Pd, completing an occupation with maximum spin, having three electrons in the 4d(t_2) states. In the case of Ag, it is only possible to place the extra electron in the 4d(t_2) spin minority state, diminishing the total spin. By their side, the 4d(e) states penetrate the fundamental band gap for Ru, and turn into resonances in the valence band for Pd and Ag. All this evolution can be followed in figure 3 in which we show the position of the 4d states relative to the band edges.

3.2. Charge distribution

In this section we analyse the charge distribution in the unit cell of the alloys. The element Y has the atomic configuration $4d5s^2$. Thus it has three valence electrons, analogously to the Ga atom, that it substitutes when forming the alloy. These three electrons integrate the valence band, constituting a closed shell electronic system, without spin polarization, and without occupied electronic states in the conduction band. As shown in figure 3 the unoccupied 4d anti-ligand states, for the GaYN alloy, lay down much higher than the CB bottom (∼12 eV). The 4d ligand states hybridize with the states of the top of the VB of GaN, mainly with the 2p

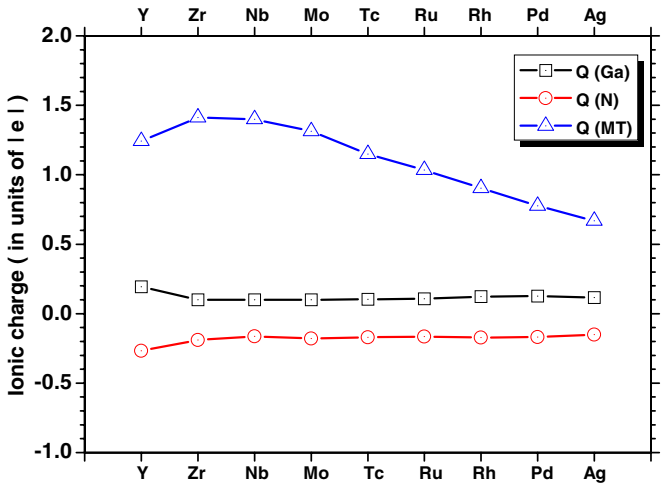

Figure 4. Evolution of the ionic charges, Q, of the atoms along the transition metal series.

N, of t_2 symmetry. As the atomic number of the TM substituting for the Ga atom increases, the 4d anti-ligand states, in the CB, decrease in energy until they reach the bottom of the CB for Tc, appear in the gap energy for Ru, and penetrate the valence band, as resonances, for Pd. In the case of Zr, in which there is the addition of one electron, with respect to Y, the occupation of electronic states occurs at the bottom of the conduction band of GaN; afterwards, for each successive TM, 4d states are occupied (first the e states and then the t_2 states), in a competition with the occupation of the states of the bottom of the conduction band to the case of Tc. From this element it starts the occupation of the localized t_2 states. In this evolution the electronic charge associated with the TM becomes more localized on it (having less charge localized in the interstitial region). In order to make an analysis of the charge distributions, as furnished by the FP-LAPW method, we adopt a semi-quantitative approach: we distribute the total charge in the intersphere region among the atomic spheres, proportionally to their volumes. We take the net charges, in each atomic sphere, as an indication of the individual atomic charges. In figure 4 we show the evolution of these charges along the series. We see that the ionicity of the pure GaN compound is practically conserved and the behaviour of the TM element is typical for a substitutional impurity in this low concentration of 6%.

3.3. Electronic configurations

An analysis of the charge distribution, inside the several atomic spheres, of the spin-polarized valence states for each angular moment component reveals the electronic configurations as displayed in table 2.

The interstitial charge labelling of the last column refers to the complementary charge, belonging to the corresponding atom, spread out in the intersphere region. For instance, the average configuration of all Ga atoms in the several compounds is Ga $3d^{9.85}4s^{0.5}4p^{0.5}$ with about 2.15 electrons in the intersphere region of the unit cell, completing the total of 13 valence electrons of the Ga atom. As we remarked before, for the alloys containing Y, Zr, Tc or Ru there is no spin polarization, the exchange splitting being, then, zero. In the other cases there are exchange splittings $\Delta E_{xc} = 0.43$ eV (Nb); 0.56 eV (Mo); 0.46 eV (Rh); 0.68 eV (Pd);

Table 2. Charge distribution in the spheres of the transition metals, in units of electron charge, per angular momentum. The last column indicates the corresponding complementary charges localized in the interstitial region. The arrows indicate the spins.

Metal	Configuration	Interstitial charge
Ga	$3d^{9.85}4s^{0.5}4p^{0.5}$	2.15
N	$2s^{1.3}2p^{2.8}$	0.90
Y	$(4p)^{5.18}(4d\ e\uparrow)^{0.06}(4d\ t_2\uparrow)^{0.28}$ $(5s)^{0.12}(4d\ e\downarrow)^{0.06}(4d\ t_2\downarrow)^{0.28}$	3.02
Zr	$(4p)^{5.46}(4d\ e\uparrow)^{0.12}(4d\ t_2\uparrow)^{0.42}$ $(4d\ e\downarrow)^{0.12}(4d\ t_2\downarrow)^{0.42}(5s)^{0.12}$	3.33
Nb	$(4d\ e\uparrow)^{0.70}(4d\ t_2\uparrow)^{0.54}(5s\uparrow)^{0.06}(5p\uparrow)^{0.15}$ $(4d\ e\downarrow)^{0.16}(4d\ t_2\downarrow)^{0.50}(5s\downarrow)^{0.06}(5p\downarrow)^{0.16}$	2.67
Mo	$(5s\uparrow)^{0.07}(4p\uparrow)^{0.12}(4d\ e\uparrow)^{1.90}(4d\ t_2\uparrow)^{0.14}$ $(5s\downarrow)^{0.06}(4p\downarrow)^{0.12}(4d\ e\downarrow)^{1.07}(4d\ t_2\downarrow)^{0.14}$	2.80
Tc	$(5s)^{0.14}(4p)^{0.19}(4d\ e\uparrow)^{1.25}(4d\ t_2\uparrow)^{0.71}$ $(4d\ e\downarrow)^{1.22}(4d\ t_2\downarrow)^{0.71}$	2.79
Ru	$(5s)^{0.16}(4p)^{0.18}(4d\ e\uparrow)^{1.42}(4d\ t_2\uparrow)^{1.03}$ $(4d\ e\downarrow)^{1.42}(4d\ t_2\downarrow)^{1.03}$	2.76
Rh	$(5s\uparrow)^{0.09}(4p\uparrow)^{0.11}(4d\ e\uparrow)^{1.53}(4d\ t_2\uparrow)^{1.82}$ $(5s\downarrow)^{0.09}(4p\downarrow)^{0.08}(4d\ e\downarrow)^{1.52}(4d\ t_2\downarrow)^{1.06}$	2.69
Pd	$(5s\uparrow)^{0.10}(4p\uparrow)^{0.13}(4d\ e\uparrow)^{1.62}(4d\ t_2\uparrow)^{2.38}$ $(5s\downarrow)^{0.10}(4p\downarrow)^{0.08}(4d\ e\downarrow)^{1.61}(4d\ t_2\downarrow)^{1.35}$	2.62
Ag	$(5s\uparrow)^{0.11}(4p\uparrow)^{0.13}(4d\ e\uparrow)^{1.70}(4d\ t_2\uparrow)^{2.52}$ $(5s\downarrow)^{0.11}(4p\downarrow)^{0.10}(4d\ e\downarrow)^{1.69}(4d\ t_2\downarrow)^{2.06}$	2.59

0.29 eV (Ag). These values are to be compared to the bigger value (3.4 eV) obtained for the $Ga_{0.94}Mn_{0.06}N$ alloy [2].

3.4. Density of states

In order to complete the study of the electronic states introduced by the 4d TM, we analyse their densities of states (figure 5). As shown in these figures, 4d TM states appear near the Fermi level, constituting impurity bands with bandwidths ∼0.6 eV (about the same as for the $Ga_{0.94}Mn_{0.06}N$ alloy [2]). These bands present exchange splittings in the cases of Nb, Mo, Rh, and Pd, which are large enough to yield high spin configurations. These states are gradually occupied as the transition metal atomic number increases. As shown in figure 6 there is a substantial hybridization between the 4d states and the 2p N from Ru to Ag. Taking into account the local symmetry at the Ga substitutional site, the 4d(t_2) orbitals have the same symmetry as the xy, xz, yz functions which hybridize with the 2p N orbital, generating ligand (L) and anti-ligand (aL) states, as shown in the diagram of figure 7. The 4d(e) orbitals have the same symmetry as the functions $3z^2 - r^2$ and $x^2 - y^2$ and extend to the interstitial region forming the non-ligand (nL) states, as also shown in figure 7. This description is common to all densities of states displayed in figure 5. For example, in the case of GaNbN, the density of the majority spin states exhibits L states and aL states around −7 and +1 eV, relative on the Fermi level, respectively. Due to their non-ligand nature, the e states appear, in this case, as a sharp peak below the Fermi level. These features may be identified in the other cases of figure 8.

Along the series, the position of the Fermi level changes, naturally, as a consequence of the addition of electrons to the system. However, due to the small concentration of the transition metal, the bandwidths and the energy gaps, between the bands, remain practically unchanged. In figure 8 we compare the total and interstitial densities of states. We see that the interstitial

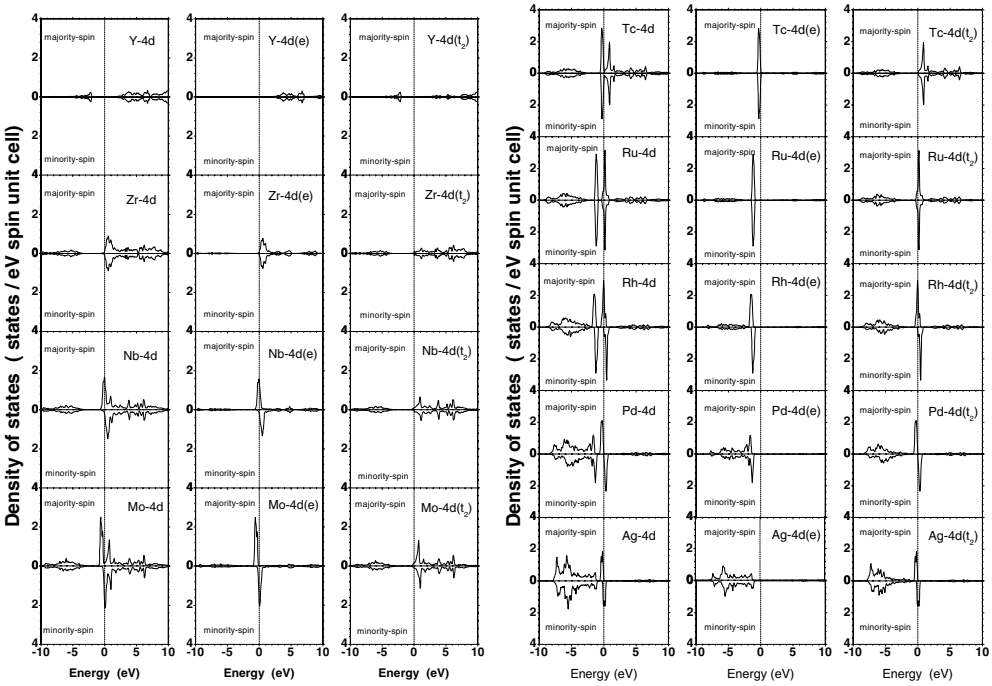

Figure 5. Partial densities of states 4d, 4d(e), and 4d(t_2) TM for the alloys. The vertical lines denote the positions of the Fermi energy.

regions make important contributions to the density of states and reflect, in each case, the degree of spatial delocalization of the electronic states. In figure 3 we summarize the evolution along the series of the energy levels introduced by the transition metals, at the Γ point, as referenced to the edges of the valence and conduction bands of GaN. We see that the 4d states start in the CB (for Y and Zr), the e states having lower energy than the t_2 states; the e states penetrate into the fundamental energy gap of GaN in the case of Ru and in the VB in the case of Pd. The t_2 states are unoccupied to Tc and remain partially occupied to the end of the series. It is interesting to note that the e and t_2 levels are imprisoned in the gap region, which can be attributed to the competition between the repulsion over these levels produced by the 4d Ga states and the attraction over the t_2 states exerted by the top of the VB.

4. Magnetic properties

The calculated magnetic moments of the Ga(4d TM)N, for each inequivalent atomic species in the unit cell are displayed in table 3. As a consequence of the spin polarization discussed before, there are large net magnetic moments for Nb ($\mu = 1.49\mu_B$), Mo ($\mu = 1.64\mu_B$) Rh ($\mu = 2.02\mu_B$), Pd ($\mu = 3.09\mu_B$), and Ag ($\mu = 2.06\mu_B$).

The main component of the cell magnetic moment is localized at the transition metal site (TM0); the additional contributions originate from the intersphere region and the N and Ga atoms located near the transition metal (TM0). The magnetic coupling between the transition metal and the first neighbours (N1) and the second neighbours (Ga2) is always ferromagnetic. We note that in the cases of Nb and Mo most of the neighbour contributions comes from the second neighbours Ga2; in the cases of Rh, Pd and Ag, the main contributions are from the first

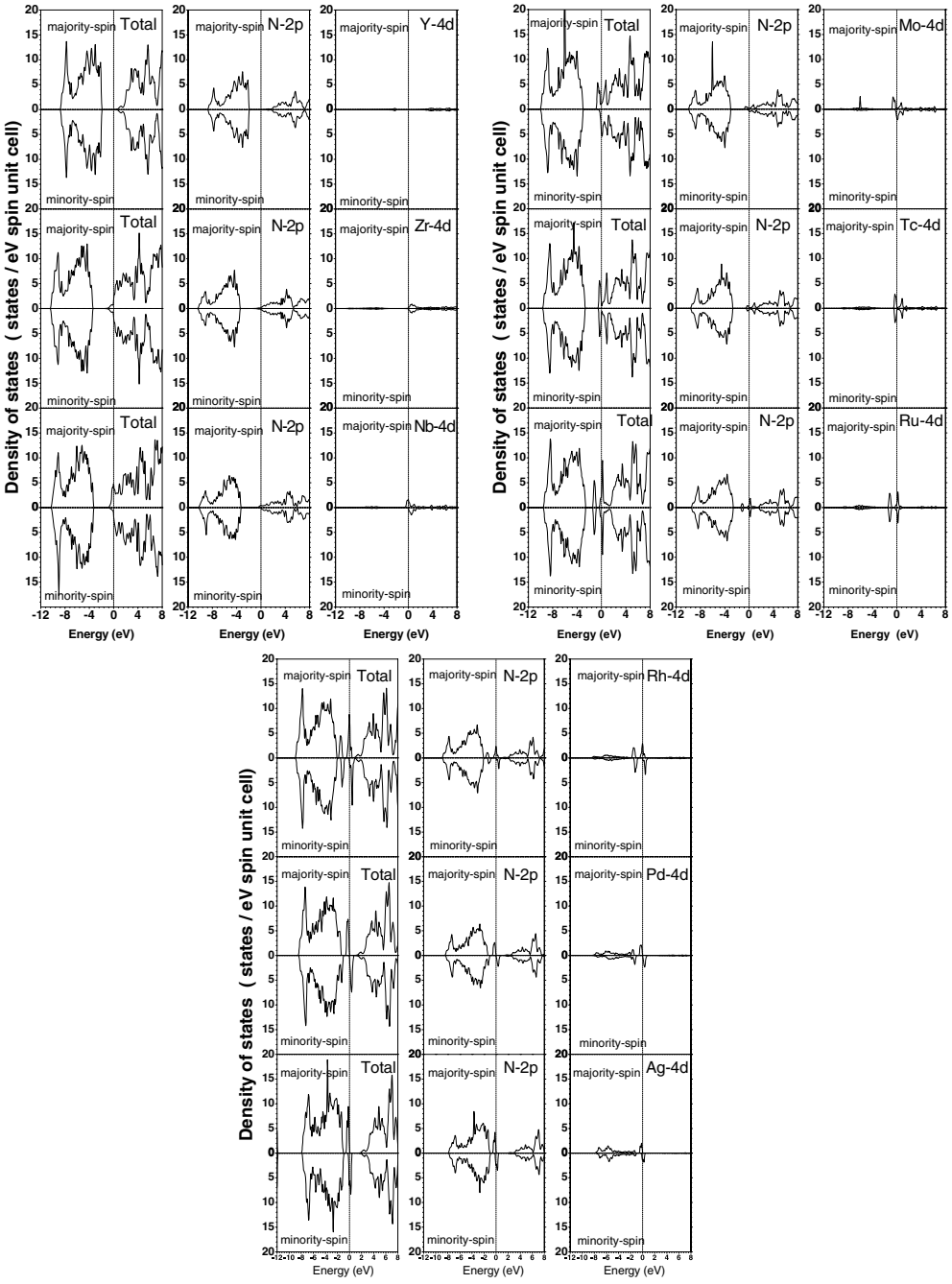

Figure 6. Total and partial densities of states (2p N and 4d TM) for the alloys. The vertical lines denote the positions of the Fermi energy.

neighbours N1. These features may be understood on the basis of the analysis we made before. In the cases of Nb and Mo, the states most responsible for the localized magnetic moments are the non-ligand 4d(e) states which do not hybridize with the 2p state of the N1 first neighbours,

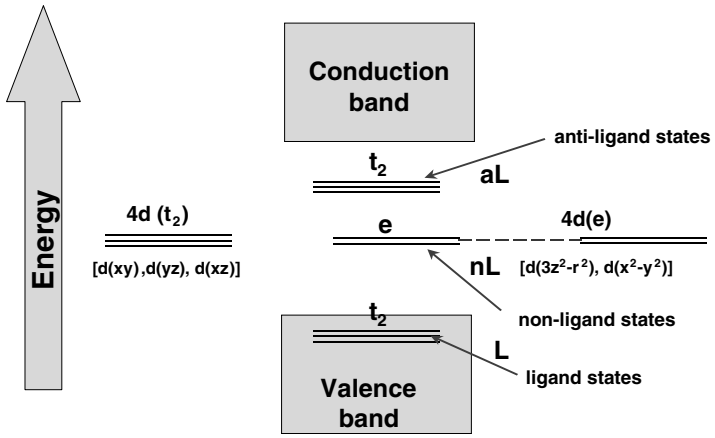

Figure 7. Energy splitting of the 4d states of the transition metal in a substitutional site of the Ga atom in the GaN. Schematically we show the t_2 ligand states (L), t_2 anti-ligand states (aL) and non-ligand states e (nL).

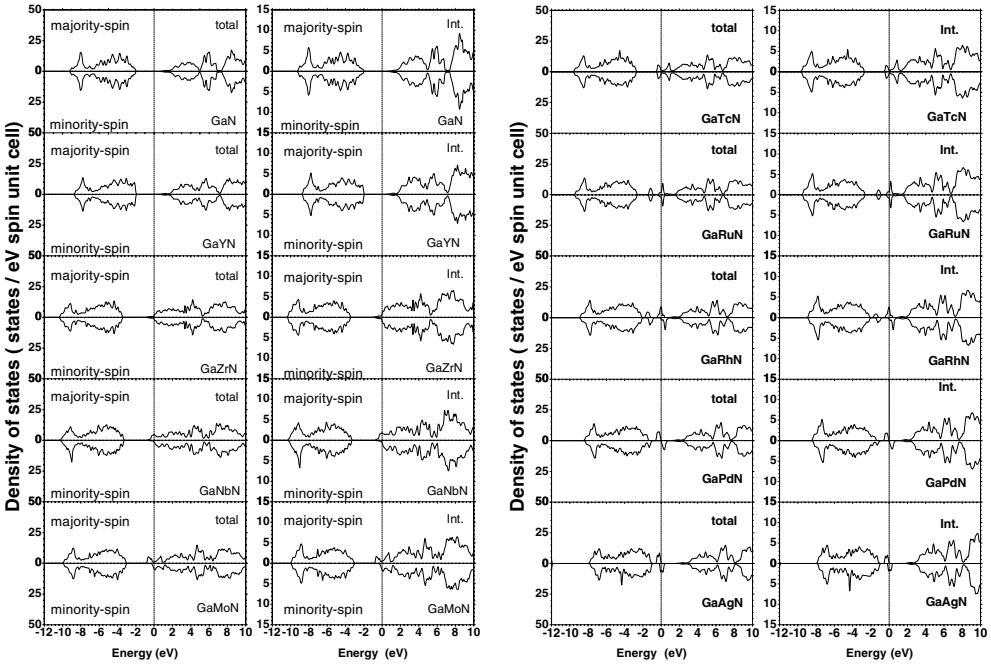

Figure 8. Total and interstitial densities of states for the alloys. The vertical lines denote the positions of the Fermi energy.

but induce a strong polarization of the second neighbours Ga2. In the cases of Rh, Pd, and Ag the states responsible for the appearance of the magnetic moments are the 4d(t_2) TM ligand states, which hybridize with the first neighbours N1, polarizing them. The drop of the magnetic moment of the cell when passing from Pd to Ag is naturally due to the addition of the 4d electron having the opposite spin to the three existing in Pd.

Table 3. Contributions to the total magnetic moment μ (in units of the Bohr magneton, μ_B) of the 32-atom supercells as determined for each non-equivalent atomic species (the multiplicity, M, refers to the number of equivalent atoms of that species in the cell). The ordering of the atoms follows the ordering of the shells of neighbours around the transition metal atom TM0 (as in figure 1, N1 means the first shell of nitrogen atoms, etc).

Atom	M	Nb	Mo	Tc	Rh	Pd	Ag
TM0	1	0.5979	0.8326	0.0357	0.8170	1.1009	0.5081
N1	4	0.0013	0.0169	0.0013	0.0988	0.2288	0.2042
Ga2	8	0.0301	0.0250	0.0006	0.0178	0.0234	0.0140
Ga3	2	0.0018	0.0013	0.0001	0.0040	0.0047	0.0024
N4	4	0.0038	0.0033	−0.0001	0.0107	0.0200	0.0222
Ga5	4	0.0009	0.0006	0.0000	0.0000	−0.0004	−0.0003
N6	8	0.0063	0.0052	0.0001	0.0095	0.0168	0.0188
Ga7	1	0.0018	0.0010	−0.0000	0.0035	0.0041	0.0028
Int.	—	0.5692	0.4845	0.0130	0.5376	0.6652	0.3742
Total	—	1.4877	1.6455	0.0593	2.0225	3.0948	2.0567

Our results show that the 4d transition metal states in the systems Ga(Nb)N, Ga(Mo)N, Ga(Rh)N, Ga(Pd)N, and Ga(Ag)N have quantitative and qualitative similarities to the 3d Mn states in the Ga(Mn)N alloy [2], except for having much smaller exchange splittings. However these splittings are extremely dependent on the lattice parameter and may be manipulated experimentally by subjecting the systems to positive and negative pressures. So, on the basis of our present study we speculate that, analogously to Ga(Mn)N, these dilute alloys may be candidates for being ferromagnetic[4] and half-metallic materials (containing a metallic majority spin system and an isolating minority spin system) when subjected to a stretching in order to separate the spin states.

The ferromagnetism of dilute magnetic semiconductors based on the 3d transition metals has been attributed to the double-exchange mechanism [5]. The key point of the stabilization of the ferromagnetic state by means of this mechanism is that there are free charge carriers. The alloys Ga(Nb)N, Ga(Mo)N, Ga(Rh)N, Ga(Pd)N, and Ga(Ag)N have non-occupied 4d states; taking into account that the electrons in occupied e states are less itinerant (because of their non-ligand character) than those occupying t_2 (aL) states, we may guess that the good candidates for being stable ferromagnetic systems are those containing t_2 (aL) states occupied by itinerant electrons, Ga(Rh)N, Ga(Pd)N, and Ga(Ag)N. Thus, the itinerant electrons occupying t_2 (aL) states would participate of the double-exchange mechanism, lowering the kinetic energy of the magnetic state, and the electrons in the e states, being more localized, would not take part in the mechanism.

5. Final remarks and conclusions

It has been demonstrated that *ab initio* calculations based on LDA can provide a reasonable discussion of the origin of the magnetism in DMS [23–25]. The calculations revealed that both the p–d exchange [26] and the double exchange [27] are important mechanisms for understanding the ferromagnetism in DMS; the relative position of the host valence band and the d states of the impurity atom determines which mechanism dominates. In the case of the $Ga_{1-x}Mn_xN$ alloy, for example, the impurity bands appear in the band gap and due to the broadening of the impurity bands the double-exchange mechanism is favoured. Thus,

[4] Very recently, the work by Osuch *et al* [33] came to our attention; in that work they obtain similar results by carrying out equivalent calculations for the wurtzite structure of the $Ga_{0.94}Pd_{0.06}N$ alloy.

the energetic position of the d states in the electronic structure is of importance to the ferromagnetism in DMS. In general, the LDA predicts occupied d states at too high energies and our results and analyses have to be considered with caution. However, even though the LDA-based description is by no means perfect, it presents, by being a first-principles approach without any phenomenological parameters, a reliable reference point for the analysis of the magnetic properties of the materials studied. As is well known, a consistent improvement of its results can be achieved only by consistently including the electron correlation in the first-principles calculations, as in Hedin's GW approach [28]. This certainly implies extremely heavy calculations, but in a broad perspective seems to be the most realistic way to proceed[5]. In this paper, we predict electronic and magnetic properties of new materials, the $Ga_{0.94}(4d\ TM)_{0.06}N$ alloys (in which the transition metal TM = Y, Zr, Nb, Mo, Tc, Ru, Rh, Pd, and Ag occupies, substitutionally, a Ga site in a GaN zinc-blende lattice). Our calculations show that in this limit of dilute doping (6%) the transition metals originate impurity energy levels which behave as resonances in the conduction band (Y, Zr, Nb, Mo, Tc: 4d(e) states; Ru, Rh: $4d(t_2)$ states); deep levels in the gap (Ru, Rh: 4d(e) states; Pd, Ag: $4d(t_2)$ states) and resonances in the valence band (Pd, Ag: 4d(e) states). Only for Nb, Mo, Rh, Pd, and Ag do local moments occur. The Ga(Rh)N, Ga(Pd)N, and Ga(Ag)N alloys are candidates for being stable ferromagnetics. The Ga(Rh, Pd)N alloy subjected to a stretching (i.e. having a lattice parameter larger than the one for equilibrium) is feasibly a half-metallic material with promising applications in spin electronics.

Acknowledgments

The authors are grateful to the Brazilian agencies CNPq (Conselho Nacional de Desenvolvimento Científico e Technológico), FAPEMIG (Fundação de Amparo à Pesquisa do Estado de Minas Gerais), and Instituto do Milênio de Nanociências for their support during the realization of this work. R de Paiva is grateful to FAPESB (Fundação de Amparo à Pesquisa do Estado de Bahia) for partial support during this work.

References

[1] Chitta V A, Coaquira J A H, Fernandez J R L, Duarte C A, Leite J R, Schikora D, As D J, Lischka K and Abramof E 2004 *Appl. Phys. Lett.* **85** 3777

Marques M, Teles L K, Scolfaro L M R, Ferreira L G and Leite J R 2004 *Phys. Rev.* B **70** 073202

Rodrigues C G, Fernandez J R L, Leite J R, Chitta V A, Freire V N, Vasconcellos A R and Luzzi R 2004 *J. Appl. Phys.* **95** 4914

Ramos L E, Furthmuller J, Leite J R, Scolfaro L M R and Bechstedt F 2003 *Phys. Rev.* B **68** 085209

[5] Many researchers believe that the LDA description can be significantly improved by combining it with the on-site Coulomb interactions, the so-called LDA + U approach [29]. The LDA + U approach introduces the empirical parameter U; therefore it is no longer a first-principles method and results depend on the choice of U. The method may give a reasonable description of the electronic structure of some systems, provided that an appropriate U value is taken. However, due to the ad hoc form of the LDA + U functional, some important details of the electronic structure of strongly correlated materials can be very wrong in LDA + U approach, which may lead to an incorrect description of interatomic magnetic interactions [30]. It can even happen that the LDA + U approach gives a much worse description for the magnetic properties than the ordinary LDA [31, 32]. With regard to the DMS $Ga_{1-x}Mn_xN$ alloy, Sato *et al* [23] have shown that the LDA + U approach does not change the electronic structure around the Fermi level so much. They were able to distinguish clear impurity bands in the energy gap both in LDA and LDA + U approaches; thus, they concluded that the main contribution to the ferromagnetism comes from the double-exchange mechanism both in the LDA and the LDA + U approaches. They found only small differences between the LDA and LDA + U calculations for the occupied states, but for the unoccupied states the d states were pushed up to higher energies in the LDA + U approach. Thus, they concluded that in the case of $Ga_{1-x}Mn_xN$ the dominant mechanism is still the double exchange.

Teles L K, Ferreira L G, Leite J R, Scolfaro L M R, Kharchenko A, Husberg O, As D J, Schikora D and Lischka K 2003 *Appl. Phys. Lett.* **82** 4274
[2] de Paiva R, Alves J L A, Nogueira R A, Leite J R and Scolfaro L M R 2005 *J. Magn. Magn. Mater.* **288** 384
[3] de Paiva R, Nogueira R A and Alves J L A 2004 *J. Appl. Phys.* **96** 6565
[4] Ohno H, Chiba D, Matsukura F, Omiya T, Abe E, Dietl T, Ohno Y and Ohtani K 2000 *Nature* **408** 944
[5] Sato K and Katayama-Yoshida H 2001 *Japan. J. Appl. Phys.* **40** L485
[6] Hohenberg P and Kohn W 1964 *Phys. Rev.* **136** B864
Kohn W and Sham L J 1965 *Phys. Rev.* **140** A1133
[7] Blaha P, Schwarz K, Madsen G K H, Kvasnicka D and Luitz J 2001 *WIEN2K—An Augmented Plane Wave & Local Orbitals Program for Calculating Crystal Properties* (Austria: Techn. Universität)
ISBN 3-9501031-1-2
[8] Ceperley D M and Alder B J 1980 *Phys. Rev. Lett.* **45** 566
[9] Perdew J P and Wang Y 1992 *Phys. Rev.* B **45** 13244
[10] Sjöstedt E, Nordström L and Singh D J 2000 *Solid State Commun.* **114** 15
[11] Madsen G K H, Blaha P, Schwarz K, Sjöstedt E and Nordström L 2001 *Phys. Rev.* B **64** 195134
[12] Vegard L 1921 *Z. Phys.* **5** 17
[13] Ohno H, Shen A, Matsukura F, Oiwa A, Endo A, Katsumoto S and Iye Y 1996 *Appl. Phys. Lett.* **69** 363
[14] Shioda R, Ando K, Hayashi T and Tanaka M 1998 *Phys. Rev.* B **58** 1100
[15] Sapega V F, Moreno M, Ramsteiner M, Daweritz L and Ploog K 2002 *Phys. Rev.* B **66** 075217
[16] Hanif K M, Meulenberg R W and Strouse G F 2002 *J. Am. Chem. Soc.* **124** 11495
[17] Jun Y-w, Jung Y-y and Cheon J 2002 *J. Am. Chem. Soc.* **124** 615
[18] Cho Y M, Choo W K, Kim H, Kim D and Ihm Y 2002 *Appl. Phys. Lett.* **80** 3358
[19] Lee H-J, Jeong S-Y, Ryong C and Park C H 2002 *Appl. Phys.* **81** 4020
[20] Jain M, Kronik L, Chelikowsky J R and Godlevsky V V 2001 *Phys. Rev.* B **64** 245205
[21] Kronik L, Jain M and Chelikowsky J R 2002 *Phys. Rev.* B **66** 041203
[22] Sanyal B, Bengone O and Mirbt S 2003 *Phys. Rev.* B **68** 205210
[23] Sato K, Dederichs P H and Katayama-Yoshida H 2006 *Physica* B **376/377** 639
[24] Sato K, Dederichs P H, Katayama-Yoshida H and Kudrnosky J 2004 *J. Phys.: Condens. Matter* **16** S5491
[25] Sato K, Schweika W, Dederichs P H and Katayma-Yoshida H 2004 *Phys. Rev.* B **70** R201202
[26] Dietl T, Ohno H, Matsukura F, Gibert J and Fernand D 2000 *Science* **287** 1019
[27] Akai H 1998 *Phys. Rev. Lett.* **81** 3002
[28] Aryasetiawan F and Gunnarsson O 1998 *Rep. Prog. Phys.* **61** 237
[29] Anisimov V L, Aryasetiawan F and Lichtenstein A L 1997 *J. Phys.: Condens. Matter* **9** 767
[30] Solovyev I V and Terakura K 1998 *Phys. Rev.* B **58** 15496
[31] Solovyev I V, Hamada N and Terakura K 1996 *Phys. Rev.* B **53** 7158
[32] Savada H, Morikawa Y, Terakura K and Hamada N 1997 *Phys. Rev.* B **56** 12154
[33] Osuch K, Lombardi E B and Adamowicz L 2005 *Phys. Rev.* B **71** 165213